Inorg. Chem. **2007**, *46*, 10365–10371

Synthesis, X-Ray, and Electronic Structures of a New Nickel Dibromide Complex. Activity in the Regioselective Catalyzed Dimerization of Ethylene into 1-Butene

Guilhem Mora, Steven van Zutphen, Christian Klemps, Louis Ricard, Yves Jean,* and Pascal Le Floch*

Laboratoire Hétéroéléments et Coordination, Ecole Polytechnique, CNRS, 91128 Palaiseau Cedex, France

Received August 1, 2007

Reaction of the bis-(3,4)-dimethylphosphole-Xanthene **1b** with [$NiBr_2$(DME)] afforded a new nickel(II) dibromide complex, **2**. Both its color and its NMR behavior change with temperature and solvent due to changes in the spin state of the complex. This led us to study the complex spin states using DFT calculations. Furthermore, the activity of **2** in catalyzed ethylene dimerization was studied, revealing both high activity and selectivity toward the production of 1-butene.

Introduction

The incorporation of phospholes in ligands for transition metal catalysts is an active area of research.[1−3] Several recent examples, including palladium, rhodium, and nickel complexes of phosphole-containing ligands, have found applications in important catalytic transformations such as hydroformylation, amine allylation, carbon−carbon bond forming reactions, or ethylene dimerization.[4−13] We recently discovered two phosphole−xanthene derivatives, DPP−Xantphos (**1a)** and DMP−Xantphos (**1b**), featuring 2,5-diphenylphosphole and 3,4-dimethylphosphole moieties as pendant arms, respectively (see Scheme 1).[14] These ligands show unusual reactivity toward palladium(II) allyl species, yielding a dimeric palladium(0) complex with **1a** and a dimeric trinuclear species with **1b**. Matt et al. studied ethylene dimerization with calixarene ligands and found that the bite angle of the ligand has an important effect on the catalyst's activity.[15] This prompted us to study our ligands, which have an unusually large bite angle, in this transformation. For this, nickel is the metal of choice.[16−19] We therefore decided to investigate the coordination behavior of ligands **1a** and **1b**

Scheme 1. Formula of Ligands **1a** and **1b**

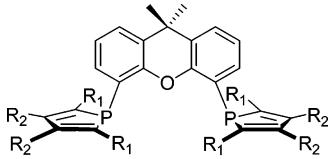

DPP-Xant: **1a** : R_1 = Ph; R_2 = H
DMP-Xant: **1b** : R_1 = H; R_2 = Me

* To whom correspondence should be addressed. E-mail: lefloch@poly.polytechnique.fr (P.L.F.); yves.jean@polytechnique.edu (Y.J.). Fax: +33-169334570 (P.L.F.). Phone: +33-169333990 (P.L.F.).

(1) Quin, L. D. *Phosphorus-Carbon Heterocyclic Chemistry: The Rise of a New Domain*; Pergamon: Amsterdam, 2001.
(2) Mathey F. *Phosphorus-Carbon Heterocyclic Chemistry: The Rise of a New Domain*, Pergamon: Amsterdam, 2001.
(3) van Zutphen, S.; Margarit, V. J.; Mora, G.; Le Floch, P. *Tetrahedron Lett.* **2007**, *48*, 2857−2859.
(4) Thoumazet, C.; Grutzmacher, H.; Deschamps, B.; Ricard, L.; le Floch, P. *Eur. J. Inorg. Chem.* **2006**, *19*, 3911−3922.
(5) Mora, G.; van Zutphen, S.; Thoumazet, C.; Le, Goff, X. F.; Ricard, L.; Grützmacher, H.; Le, Floch, P. *Organometallics* **2006**, *25*, 5528−5532.
(6) Thoumazet, C.; Ricard, L.; Grutzmacher, H.; le Floch, P. *Chem. Commun.* **2005**, 1592−1594.
(7) Thoumazet, C.; Melaimi, M.; Ricard, L.; Mathey, F.; le Floch, P. *Organometallics* **2003**, *22*, 1580−1581.
(8) Melaimi, M.; Thoumazet, C.; Ricard, L.; le Floch, P. *J. Organomet. Chem.* **2004**, *689*, 2988−2994.
(9) Cortes, J. G. L.; Ramon, O.; Vincendeau, S.; Serra, D.; Lamy, F.; Daran, J-C.; Manoury, E.; Gouygou, M. *Eur. J. Inorg. Chem.* **2006**, *24*, 5148−5157.
(10) Holz, J.; Gensow, M. N.; Zayas, O.; Boerner, A. *Curr. Org. Chem.* **2007**, *11*, 61−106.
(11) Mourgues, S.; Serra, D.; Lamy, F.; Vinceandeau, S.; Daran, J.-C.; Manoury, E.; Gouygou, M. *Eur. J. Inorg. Chem.* **2003**, 2820−2826.
(12) de Souza, R. F.; Bernardo-Gusmao, K.; Cunha, G. A.; Loup, C.; Leca, F.; Réau, R. *J. Catal.* **2004**, 235−239.
(13) (a) Vogt, D. *Applied Homogeneous Catalysis with Organometallic Compounds*; Wiley: Weinhein, 1996. (b) Chauvin, Y.; Olivier, H. ibid.
(14) Mora, G; Deschamps, B; van Zutphen, S; Le Goff, X. F; Ricard, L; Le Floch, P *Organometallics* **2007**, *26*, 1846−1855.
(15) Lejeune, M.; Sémeril, D.; Jeunesse, C.; Matt, D.; Peruch, F.; Lutz, P. J.; Ricard, L. *Chem. Eur. J.* **2004**, *10*, 5354−5360.

10.1021/ic701529a CCC: $37.00
Published on Web 10/26/2007

Scheme 2. Reaction of **1b** with [$NiBr_2$(DME)] to Form Complex **2**

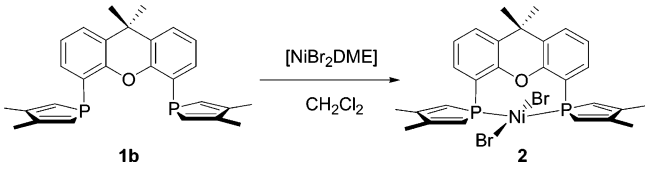

with $NiBr_2$ and study the reactivity of these complexes in ethylene dimerization. We here report the synthesis and theoretical analysis of the spin states of the nickel(II) DMP−Xantphos complex, as well as its activity in the ethylene dimerization reaction.

Results and Discussion

a. Syntheses of Complexes 2, 5, and 6 and Their ^{31}P NMR Behavior. Synthesis of dibromide nickel complexes was carried out by reacting the [$NiBr_2$(DME)] (DME = dimethoxyethane) complex with ligands **1a** and **1b** in dichloromethane at room temperature. Whereas a clean and rapid reaction took place with ligand **1b**, yielding complex **2** (see Scheme 2), no reaction occurred with the tetraphenyl ligand **1a**. Whatever the experimental conditions used (heating, prolonged reaction time, solvent = tetrahydrofuran (THF), acetonitrile, toluene), work up exclusively led to recovery of the starting materials.

The characterization of complex **2** was not straightforward. Indeed, no ^{1}H or ^{31}P NMR signal is visible at room temperature, suggesting a paramagnetic behavior. This observation is consistent with d^8 Ni(II) complexes adopting a tetrahedral geometry. However, when the temperature was decreased to −40 °C, the ^{31}P NMR spectrum revealed the presence of a very broad signal ($\nu_{1/2}$ = 840 Hz) around 0 ppm, which then progressively sharpened upon further cooling. At −80 °C, the ^{31}P NMR spectrum exhibited a singlet at 4.3 ppm ($\nu_{1/2}$ = 98 Hz), indicative of a singlet ground state. Moreover, during the same NMR experiment, the solution of **2** in dichloromethane turned from dark blue at room temperature to pale violet at low temperature (−80 °C), suggesting a change of the spin state. Note that this phenomenon was found to be reversible. Unfortunately, no clear ^{1}H NMR data could be recorded even at low temperature; only broad indistinct signals were observed.

Fortunately, suitable crystals for a X-ray structure determination were obtained by slow diffusion of a mixture of hexanes into a dichloromethane solution of complex **2** at room temperature. A view of one molecule of complex **2** is presented in Figure 1, and the most relevant metric parameters are listed in the corresponding legend. Crystal data and structural refinement details are presented in Table 1.

As can be seen, contrary to what might be expected from ^{31}P NMR data recorded at room temperature, complex **2** adopts a ML_5 square-based pyramidal conformation. The two phosphole moieties are coordinated in a mutual trans fashion and the oxygen atom of the xanthene is pointing toward the metal in the apical position. However, 2.481(1)Å for the Ni−O bond appears to be too long to consider that real bonding takes place. A similar coordination mode has been observed before for [$NiBr_2$(4,5-bis{di[(2-*tert*-butyl)phenyl]-phosphonito}-9,9-dimethylxanthene].[20] The observed bite angle P1−Ni−P2 of complex **2** is 158.74(2)°, while the angle Br1−Ni−Br2 is 173.84(1)°. Complex **2** must therefore be regarded as a square-planar complex in which a very weak interaction takes place with the oxygen atom. Note that, in general, nickel complexes with coordinated ether moieties show an average Ni−O bond length of 2.15 Å.[21]

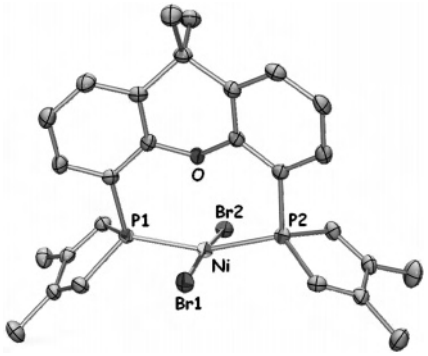

Figure 1. View of one molecule of **2**. Thermal ellipsoids are drawn at the 30% probability level. Hydrogen atoms are omitted for clarity. Selected bond distances (Å) and angles (deg): Ni−P(2), 2.192(1); Ni−P(1), 2.2035-(5); Ni−Br(2), 2.3028(3); Ni−Br(1), 2.3265(3); Ni−O, 2.481(1); P(1)−Ni−P(2), 158.74(2); P(2)−Ni−Br(2), 92.11(2); P(1)−Ni−Br(2), 93.58(2); P(2)−Ni−Br(1), 88.71(2); P(1)−Ni−Br(1), 87.81(2); Br(2)−Ni−Br(1), 173.84(1); O−Ni−P(2), 80.24(3); O−Ni−P(1), 78.82(3); O−Ni−Br(2), 95.68(3); O−Ni−Br(1), 90.48(3).

Solvent effects on the electronic structure of **2** were studied. The most significant result was obtained when dissolving complex **2** in THF. At room temperature, the mixture color was found to be unchanged (dark blue), suggesting that no coordination of the solvent had taken place. However, at low temperature (−80 °C), the solution slowly turned to green, and contrary to what was previously observed with CH_2Cl_2 solutions of **2**, no ^{31}P NMR signal could be observed. This observation led us to propose that, at low temperature, a new complex (**3**) with a coordinated THF in the second apical position is formed. This process was found to be fully reversible. Several examples of Ni(II) in the presence or absence of coordinating solvent have been studied before, and it was concluded that the decrease of temperature in the presence of a coordinating solvent transforms a square-planar singlet into an octahedral triplet.[22−23] (Scheme 3). Unfortunately, despite many attempts, no crystals of complex **3** could be obtained at low temperature. Though the structure proposed is hypothetical, DFT calculations presented confirm this hypothesis.

(16) Speiser, F.; Braunstein, P.; Saussine, L. *Acc. Chem. Res.* **2005**, *38*, 784−793, and references herein.
(17) Sauthier, M.; Leca, F.; de Souza, R. F.; Bernardo-Gusmao, K.; Queiroz, L. F. T.; Toupet, L.; Reau, R. *New J. Chem.* **2002**, *26*, 630−635.
(18) Weng, Z. Q.; Teo, S.; Koh, L. L.; Hor, T. S. A. *Chem. Commun.* **2006**, 1319−1321.
(19) Ajellal, N.; Kuhn, M. C. A.; Boff, A. D. G.; Horner, M.; Thomas, C. M.; Carpentier, J.-F.; Casagrande, O. L. *Organometallics* **2006**, *25*, 1213−1216.
(20) Van, der Vlugt, J. I.; Hewat, A. C.; Neto, S.; Sablong, R.; Mills, A. M.; Lutz, M.; Spek, A. L.; Müller, C.; Vogt, D. *Adv. Synth. Catal.* **2004**, *346*, 993−1003.
(21) Allen, F. H.; Kennard, O. *Chem. Des. Autom. News* **1993**, *8*, 31.
(22) Ohtsu, H.; Tanaka, K. *Inorg. Chem.* **2004**, *43*, 3024−3030.
(23) Boiocchi, M.; Fabbrizzi, L.; Foti, F.; Vazquez, M. *Dalton Trans.* **2004**, 2616−2620.

Table 1. Crystal Data and Structural Refinement Details for **2** and **5**

compound	**2**	**5**
cryst size [mm^3]	0.26 × 0.16 × 0.10	0.18 × 0.08 × 0.04
empirical formula	$C_{27}H_{28}Br_2NiOP_2$	$C_{39}H_{32}Br_2NiOP_2$,0.5(C_7H_8),0.5(CH_2Cl_2)
molecular mass	648.96	885.65
cryst syst	monoclinic	triclinic
space group	$P2_1/c$	$P\bar{1}$
a [Å]	10.5190(10)	9.504(1)
b [Å]	18.0280(10)	10.503(1)
c [Å]	13.7460(10)	19.600(1)
α [deg]	90.00	84.716(1)
β [deg]	92.8900(10)	89.498(1)
γ [deg]	90.00	74.856(1)
V [Å^3]	2603.4(3)	1880.3(3)
Z	4	2
calcd density [g cm^{-3}]	1.656	1.564
abs coeff [cm^{-1}]	3.956	2.831
θ_{max} [deg]	30.03	26.02
F(000)	1304	896
index ranges	$-14 \le h \le 11$	$-10 \le h \le 11$
	$-23 \le k \le 25$	$-12 \le k \le 12$
	$-18 \le l \le 19$	$-24 \le l \le 21$
reflns collected/independent	24 900/7590	17 225/7367
reflns used	5621	4859
(R_{int})	0.0288	0.0414
abs corr	0.4261 min,	0.6297 min,
	0.6931 max	0.8952 max
params refined	304	475
reflns/param	18	10
final R1[a]/wR2 [$I > 2\sigma(I)$][b]	0.0287/0.0689	0.0409/0.0921
GOF on F^2	0.995	0.975
diff. peak/hole [e Å^{-3}]	0.415(0.080)/−0.475(0.080)	0.902(0.090)/−1.025(0.090)

[a] $R1 = \sum||F_o| - |F_c||/\sum|F_o|$. [b] $wR2 = (\sum w||F_o| - |F_c||^2/\sum w|F_o|^2)^{1/2}$.

Scheme 3. Thermochromic Equilibrium of Complex **2**

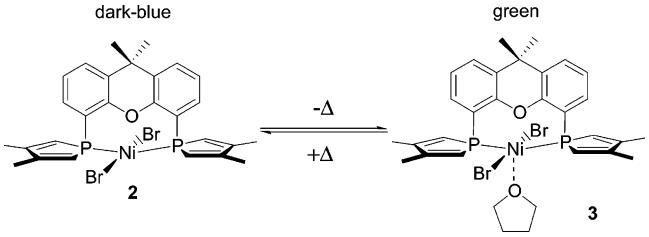

Scheme 4. Synthesis of Complex **5**

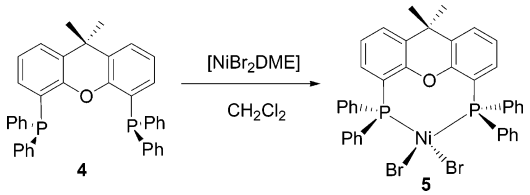

To complete our study on the electronic structure of these systems, we synthesized [$NiBr_2$(Xantphos)] (**5**) (Xantphos = 9,9-dimethyl-4,5-bis(diphenylphosphino)xanthene, **4**) (Scheme 4) and [$NiBr_2$(DMP)] (**6**) (DMP = 1-phenyl-3,4-dimethylphosphole). Complex **5** was prepared by adding 1 equiv of the Xantphos ligand (**4**) to a solution of [$NiBr_2$(DME)] in dichloromethane. The solution turned green instantaneously, indicative of the coordination taking place.

Complex **5** was found to be NMR silent due to it being paramagnetic. Importantly, recording the ^{31}P NMR spectra at low temperature or replacement of CH_2Cl_2 by THF did not induce the appearance of a signal. We therefore concluded that the structure of **5** and its spin-state configuration were maintained whatever the temperature. The structure proposed for **5** was confirmed by an X-ray crystal analysis. Diffusion of toluene in a solution of **5** in dichloromethane yielded crystals whose structure revealed a tetrahedral geometry. A view of one molecule of **5** is presented in Figure 2, and the most significant parameters are listed in the corresponding legend. Crystal data and structural refinement details are presented in Table 1.

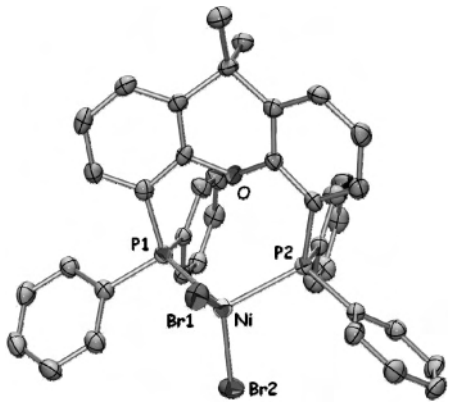

Figure 2. View of one molecule of **5**. Thermal ellipsoids are drawn at the 30% probability level. Hydrogen atoms are omitted for clarity. Selected bond distances (Å) and angles (deg): Ni−P(2), 2.323(1); Ni−P(1), 2.333(1); Ni−Br(2), 2.342(1); Ni−Br(1), 2.347(1); Ni−O, 3.222(2); P(1)−Ni−P(2),108.00(4); P(2)−Ni−Br(2), 103.93(3); P(1)−Ni−Br(2), 106.02(3); P(2)−Ni−Br(1), 105.58(3); P(1)−Ni−Br(1), 102.88(3); Br(2)−Ni−Br(1), 129.20(3); P(2)−Ni−O, 58.58(4); P(1)−Ni−O, 58.24(4); Br(2)−Ni−O, 143.04(5); Br(1)−Ni−O, 87.76(4).

In the case of DMP, the well-defined complex **6** resulting from the coordination of two DMP units onto the $NiBr_2$ fragment was readily prepared by reaction of 2 equiv of the ligand with [$NiBr_2$(DME)] in CH_2Cl_2 at room temperature. The ^{31}P NMR spectrum of **6** is characterized by a broad

Scheme 5. Synthesis of Complex **6**

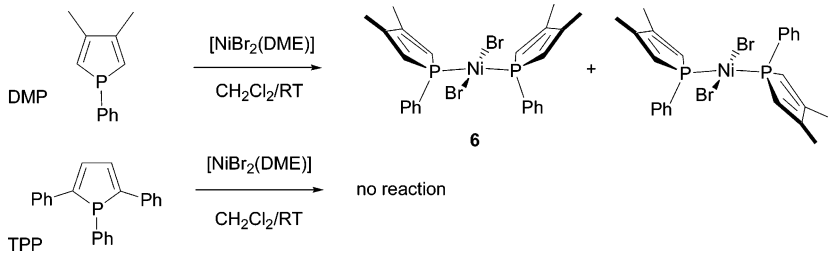

signal at room temperature but showed two different signals when the temperature was decreased (δ 18.1 ppm 2.2 times more intense than δ 29.5 ppm, determined at −80 °C). These results could be rationalized when **6** was structurally characterized by monocrystal X-ray diffraction (see Supporting Information) which showed two different structures with the phospholes moieties syn or anti (see Scheme 5). The hindered rotation of the phosphole ligand causes a broad signal.

Less satisfactory results were obtained with the TPP ligand (TPP = 1,2,5-triphenylphosphole), which was found to be reluctant toward coordination with the $NiBr_2$ fragment, all experiments yielding the starting materials whatever the experimental conditions used (see Scheme 5).

b. Theoretical Study of Complexes 2, 3, and 5. All these results prompted us to launch a theoretical study of the DMP−xantphos and xantphos nickel dibromide complexes **2**, **3**, and **5**. DFT calculations with the B3PW91 functional were performed for both the singlet and the triplet states. In these calculations, the four methyl groups of the phosphole moieties (complexes **2** and **3**) and the two methyl groups of the xanthene backbone (complexes **2**, **3**, and **5**) were replaced by H atoms (see the Experimental Section for further details regarding these calculations).

The optimized geometry for the singlet state of complex **2** (see Figure 3, the more significant metric parameters being listed in the corresponding legend) was found to be in good agreement with the X-ray structure. It can therefore be described as a d^8 ML_5 square-based pyramidal complex with an elongated apical bond (Ni−O = 2.51 Å (exptl, 2.481(1) Å)). The metal−ligand bond lengths are overestimated by 0.02−0.05 Å, and bond angles around the metal center are reproduced within 2−3°. Optimization of the triplet state led to a very different structure (see Figure 4, the more significant metric parameters being listed in the corresponding legend). The oxygen center is no longer bound to the metal (Ni−O = 3.33 Å), and a distorted tetrahedral arrangement was found for the remaining ML_4 unit, with P−Ni−P = 111.3° and Br−Ni−Br = 143.6°. On geometrical grounds (comparison with the X-ray structure), a singlet ground state is thus predicted for complex **2**. However, on energetic grounds, the triplet state was found to be slightly more stable than the singlet state, by 2.4 kcal mol^{-1}. This result is consistent neither with the X-ray structure nor with the NMR data at low temperature. However, it must be considered with caution since it is well known that in the DFT framework the energy ordering of low-spin and high-spin states of a given system may depend on the functional.[24] The NMR data at low-temperature prove that the singlet state is actually the electronic ground state. On the other hand, calculations suggest the existence of a low-lying triplet state, suggesting a mixture of spin states in solution at room temperature. The dark blue color could therefore be the result of the mixture of the pale violet singlet and dark blue triplet states. It has not been possible to crystallize complex **2** in its tetrahedral geometry. Apparently this conformation is not favored in the solid state.

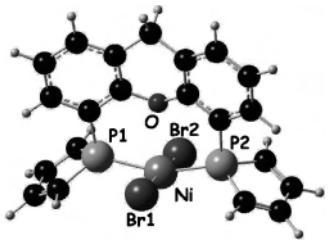

Figure 3. Singlet state of **2**. Relevant bond distances (Å) and bond angles (deg): Ni−P(2), 2.24; Ni−P(1), 2.24; Ni−Br(2), 2.33; Ni−Br(1), 2.35; Ni−O, 2.51; P(1)−Ni−P(2), 156.8; Br(2)−Ni−Br(1), 176.1.

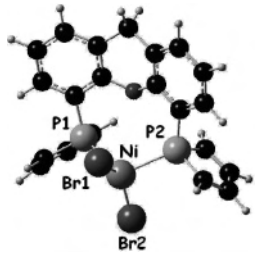

Figure 4. Triplet state of **2**. Relevant bond distances (Å) and bond angles (deg): Ni−P(2), 2.41; Ni−P(1), 2.41; Ni−Br(2), 2.35; Ni−Br(1), 2.37; Ni−O, 3.33; P(1)−Ni−P(2), 111.3; Br(2)−Ni−Br(1), 143.6.

DFT calculations were also carried out on complex **2** in interaction with a THF solvent molecule (complex **3**). The theoretical structures are given in Figures 5 and 6, and the most relevant metric parameters are listed in the corresponding legends. Both structures can be described as distorted octahedral d^8 ML_6 complexes. The triplet state is found to be more stable than the singlet state by 12.1 kcal mol^{-1}, a large energy gap which rationalizes the absence of NMR signal in THF even at low temperature. According to the d^8 electronic configuration, two electrons are lying in the two orbitals derived from the e_g block of an ideal octahedron. In going from the singlet to the triplet state, one electron of z^2 (mainly Ni−O and Ni−O_{THF} antibonding) is transferred to x^2-y^2 (mainly Ni−Br and Ni−P antibonding) so that Ni−O and Ni−O_{THF} are reinforced whereas Ni−Br and Ni−P are

(24) Zein, S; Borshch, S. A.; Fleurat-Lessard, P; Casida, M. E.; Chermette, H. *J. Chem. Phys.* **2007**, *126*, 014105.

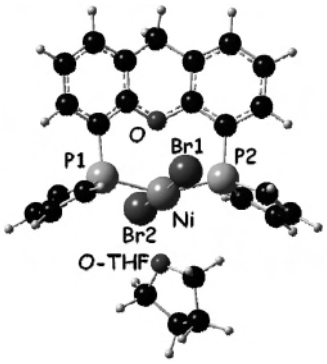

Figure 5. Singlet state of complex **3**. Relevant bond distances (Å) and bond angles (deg): Ni−P(2), 2.25; Ni−P(1), 2.25; Ni−Br(2), 2.36; Ni−Br(1), 2.37; Ni−O, 2.60; Ni−O_{THF}, 2.55; P(1)−Ni−P(2), 152.7; Br(2)−Ni−Br(1), 173.9.

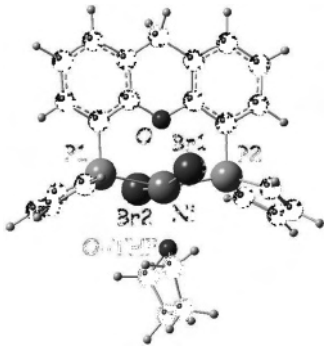

Figure 6. Triplet state of complex **3**. Relevant bond distances (Å) and bond angles (deg): Ni−P(2), 2.39; Ni−P(1), 2.39; Ni−Br(2), 2.52; Ni−Br(1), 2.52; Ni−O, 2.35; Ni−O_{THF}, 2.12; P(1)−Ni−P(2), 159.2; Br(2)−Ni−Br(1), 166.7.

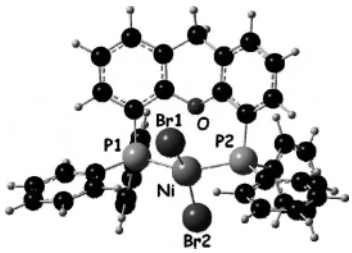

Figure 7. Singlet state of complex **5.** Relevant bond distances (Å) and bond angles (deg): Ni−P(2), 2.26; Ni−P(1), 2.26; Ni−Br(2), 2.31; Ni−Br(1), 2.37; Ni−O, 2.66; P(1)−Ni−P(2), 149.4; Br(2)−Ni−Br(1), 156.4.

weakened (the orbitals are presented in the Supporting Information).

Finally, geometry optimizations were performed for both the singlet and the triplet state of the [$NiBr_2$(Xantphos)] complex, **5**. The theoretical structures are presented in Figures 7 and 8, and the most relevant metric parameters are listed in the corresponding legends. For the triplet state, there is little change with respect to the related [$NiBr_2$(DMP-Xantphos)] complex, **2**, a pseudo-tetrahedral arrangement being found for both complexes. In contrast, a large geometrical change occurs in the singlet state. The near square-planar arrangement of the $NiBr_2P_2$ unit in **2** (Br−Ni−Br = 176.1° and P−Ni−P = 156.8°) evolves toward a pseudo-tetrahedral geometry in **5** (Br−Ni−Br = 156.4° and P−Ni−P = 149.4°), leading to a further lengthening of the Ni−O bond (2.66 instead of 2.61 Å). These geometrical evolutions in

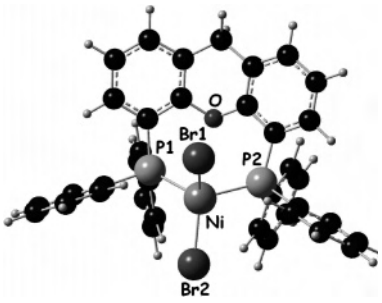

Figure 8. Triplet state of complex **5.** Relevant bond distances (Å) and bond angles (deg): Ni−P(2), 2.41; Ni−P(1), 2.41; Ni−Br(2), 2.38; Ni−Br(1), 2.39; Ni−O, 3.24; P(1)−Ni−P(2), 111.1; Br(2)−Ni−Br(1), 135.8.

going from **2** to **5** can be rationalized by the presence of sterically encumbering PPh_2 ligands in **5** which favors a pseudo-tetrahedral arrangement. It thus imposes a large geometrical distortion for the singlet state while the geometry of the triplet state is left almost unchanged. The destabilization of the singlet state by steric interactions is also reflected by the evolution of the singlet−triplet energy gap which increases from 2.4 to 14.4 kcal mol^{-1}. The triplet state is now by far the most stable, a result consistent with the NMR data.

c. Reactivity of Complexes 2, 5, and 6 in the Catalyzed Oligomerization of Ethylene. The catalytic activities of complexes **2**, **5**, and **6** were evaluated in the oligomerization of ethylene to form α-olefins. All reactions were carried out following a procedure which is detailed in the Experimental Section. Reactions were conducted in toluene at 20 °C in the presence of MAO (methylaluminoxane) as co-catalyst (300 equiv) under an ethylene pressure of 30 bar. Reactions were stopped after 30 min, and the amounts of butenes and hexenes formed were evaluated by GC analysis. In order to determine the effect of the ligand on catalyst selectivity and activity, [$NiBr_2$(DME)] was evaluated.

Results of the catalytic experiments are reported in Table 2. Nickel-based systems bearing bidentate P,[15] N,[17] and P,N[12] ligands have previously been evaluated in ethylene oligomerization. Sauthier et al. reported activities of up to 135 000 mol(C_2H_4) × mol^{-1}[Ni] × h^{-1} with a 1,2-diiminophosphoranyl nickel catalyst; however, the α-selectivity in the butenes fraction is as low as 17% and a significant portion (11%) of higher olefins (>C6) are produced.[17] A series of 2-pyridylphosphole nickel complexes were tested by de Souza et al. in the ethylene oligomerization reaction and activities of up to 56 150 mol(C_2H_4) × mol^{-1}[Ni] × h^{-1} were observed with a tight C4-centered product distribution and α-selectivities of 2−80% within the butenes fraction.[12] Taking the activity and selectivity of [$NiBr_2$(DME)] as a reference point, it can be observed that addition of TPP or DMP only slightly changes the activity but reduces the selectivity toward 1-butene from 85% to 30−40%. Even though complex **6** exhibits a good selectivity toward the formation of 1-butene (97% in 1-C4), its activity is substantially decreased compared to [$NiBr_2$(DME)]. The [$NiBr_2$(Xantphos)] complex, **5**, shows an activity and selectivity pattern almost identical to [$NiBr_2$(DME)] which suggests that decoordination of the ligand may occur during catalysis. As mentioned above, no

Table 2. Catalytic Results in Ethylene Oligomerization

catalyst[a]	% C4	%1-C4	% C6	%1-C6	% C8	%1-C8	TOF mol(C_2H_4) × mol^{-1} [Ni] × h^{-1}
2	97	90	3	56	Tr.	−	43 000
5	96	88	4	34	Tr.	−	14 000
6	93	97	7	26	Tr.	−	900
[$NiBr_2$(DME)] + DMP[b]	93	40	7	20	Tr.	−	11 000
[$NiBr_2$(DME)] + TPP[b]	92	34	8	15	Tr.	−	15 000
[$NiBr_2$(DME)] + **1a**[b]	94	66	6	21	Tr.	−	1000
[$NiBr_2$(DME)]	94	85	6	29	Tr.	−	15 000

[a] Conditions: T = 20 °C, 30 bar C_2H_4, 0.5 h, 8 μmol Ni complex, 300 equiv of MAO, solvent: toluene (20 mL) (Tr. = traces). [b] 1.7 mol equiv of ligand per mole of [$NiBr_2$(DME)].

coordination of **1a** to [$NiBr_2$(DME)] was observed. Catalytic testing of an in situ prepared mixture of [$NiBr_2$(DME)] and **1a** gave a C4/C6 ratio identical to the one obtained with [$NiBr_2$(DME)] only, but the overall activity decreased dramatically and selectivity toward 1-butene was reduced to 66%. Finally, more encouraging results were obtained with complex **2**, which exhibits almost three-fold better activity than [$NiBr_2$(DME)] along with a considerably better selectivity toward 1-butene (90% in 1-C4). It should be noted that formation of neither oligomeric products of higher molecular mass (>C8) nor polymeric material were observed in any of these catalytic experiments.

In summary, a new nickel (II) dibromide complex (**2**) has been synthesized. Its high-spin and low-spin states pertain to levels of comparable energy and either the presence of a coordinating solvent or the change of temperature can favor one state with respect to the other. Moreover, **2** appeared to be particularly active and selective in the catalyzed dimerization of ethylene into 1-butene.

Experimental Section

Synthesis. All reactions were routinely performed under an inert atmosphere of argon or nitrogen using Schlenk and glovebox techniques and dry deoxygenated solvents. Dry hexanes and THF were obtained by distillation from Na/benzophenone. Dry dichloromethane was distilled on P_2O_5, and dry toluene on metallic Na. Nuclear magnetic resonance spectra were recorded on a Bruker AC-300 SY spectrometer operating at 121.5 MHz for ^{31}P. ^{31}P chemical shifts are relative to a 85% H_3PO_4 external reference. The following abbreviation is used: s, singlet. **1a**, **1b,**[14] [$NiBr_2$(DME)],[25] **4**,[26] 1,2,5-triphenylphosphole (TPP),[27] and 1-phenyl-3,4-dimethylphosphole (DMP)[28] were prepared according to literature procedures. All other reagents and chemicals were obtained commercially and used as received. Elemental analyses were performed by the "Service d'analyse du CNRS", at Gif sur Yvette, France. The GC yields were determined on a PERICHROM 2100 gas chromatograph equipped with a HP PONA column (50 m × 202 μm, 0.5 mm film).

Synthesis of Complex 2 [$NiBr_2$DMP-Xantphos]. To a solution of [$NiBr_2$(DME)] (DME = dimethoxyethane) (50 mg, 0.162 mmol) in 5 mL of dichloromethane was added 69.7 mg (0.162 mmol) of DMP−Xantphos. An immediate color change to dark blue was observed. The solvent was removed in vacuo, and the residue triturated with petroleum ether (2 × 3 mL) to yield 97.8 mg (0.151 mmol, 93%) of [$NiBr_2$(DMP-Xantphos)] as a blue powder. ^{31}P{^{1}H} NMR (CH_2Cl_2, −80 °C): δ 4.3 (s); Anal. Calcd for $C_{27}H_{28}Br_2NiOP_2$: C, 49.97; H, 4.35. Found: C, 49.51; H, 4.32.

Synthesis of Complex 5 [$NiBr_2$Xantphos]. [$NiBr_2$(DME)] (50 mg, 0.162 mmol) was added to a solution of 94.0 mg (0.162 mmol) of Xantphos in 5 mL of dichloromethane. An immediate color change to green was observed. The reaction mixture was stirred for 12 h, the solvent was removed in vacuo, and the residue triturated with petroleum ether (2 × 3 mL) to yield 107 mg (0.134 mmol, 83%) of [$NiBr_2$(Xantphos)] as a green powder. Due to the paramagnetic nature of the complex, no characterization by NMR was possible. Anal. Calcd for $C_{39}H_{32}Br_2NiOP_2$: C, 58.76; H, 4.05. Found: C, 58.65; H, 4.08.

Synthesis of Complex 6 [$NiBr_2DMP_2$]. [$NiBr_2$(DME)] (41 mg, 0.1333 mmol) was added to a solution of 50 μL (0.266 mmol) of 3,4-dimethyl-1-phenyl-1*H*-phosphole (DMP) in 5 mL of dichloromethane. An immediate color change from transparent to brown was observed. The reaction mixture was stirred for 1 h, the solvent was removed in vacuo, and the residue triturated with petroleum ether (2 × 3 mL) to yield 64 mg (0.108 mmol, 81%) of [$NiBr_2$-$(DMP)_2$] as a brown powder. ^{31}P{^{1}H} NMR (CH_2Cl_2, −80 °C): δ 18.1 (s), 29.5 (s) for the two conformations (see Supporting Information for X-ray structures). Anal. Calcd for $C_{24}H_{26}Br_2NiP_2$: C, 48.45; H, 4.41. Found: C, 48.61; H, 4.46.

General Procedure for the Catalyzed Dimerization of Ethylene. All catalytic reactions were carried out in a magnetically stirred 120 mL stainless steel autoclave, equipped with a pressure gauge and needle valves for injections. The interior of the autoclave was protected from corrosion by a Teflon protective coating and a glass liner. A typical reaction was performed by introducing in the reactor under nitrogen atmosphere the nickel complex (8 μmol) and 20 mL of toluene. After injection of the MAO solution (300 equiv), the reactor was immediately brought to the desired working pressure and continuously fed by ethylene using a reserve bottle.

(25) King, R. B. Academic Press: New York 1965.
(26) (a) Kranenburg, M.; van der Burgt, Y. E. M.; Kamer, P. C. J.; van Leeuwen, P. W. N. M.; Goubitz, K.; Fraanje, J. *Organometallics* **1995**, *14*, 3081−3089. (b) Hillebrand, S.; Bruckmann, J.; Krüger, K.; Haenel, M. W. *Tetrahedron Lett.* **1995**, *36*, 75−78.
(27) Campbell, I. G.; Cookson, R. C.; Hocking, M. B.; Hughes, A. N. *J. Chem. Soc.* **1965**, 2184−2193.
(28) Breque, A; Mathey, F; Savignac, P. *Synthesis-Stuttgart* **1981**, 983−985.
(29) Frisch, M. J.; Trucks, G. W.; Schlegel, H. B.; Scuseria, G. E.; Robb, M. A.; Cheeseman, J. R.; Montgomery, J. A., Jr.; Vreven, T.; Kudin, K. N.; Burant, J. C.; Millam, J. M.; Iyengar, S. S.; Tomasi, J.; Barone, V.; Mennucci, B.; Cossi, M.; Scalmani, G.; Rega, N.; Petersson, G. A.; Nakatsuji, H.; Hada, M.; Ehara, M.; Toyota, K.; Fukuda, R.; Hasegawa, J.; Ishida, M.; Nakajima, T.; Honda, Y.; Kitao, O.; Nakai, H.; Klene, M.; Li, X.; Knox, J. E.; Hratchian, H. P.; Cross, J. B.; Bakken, V.; Adamo, C.; Jaramillo, J.; Gomperts, R.; Stratmann, R. E.; Yazyev, O.; Austin, A. J.; Cammi, R.; Pomelli, C.; Ochterski, J. W.; Ayala, P. Y.; Morokuma, K.; Voth, G. A.; Salvador, P.; Dannenberg, J. J.; Zakrzewski, V. G.; Dapprich, S.; Daniels, A. D.; Strain, M. C.; Farkas, O.; Malick, D. K.; Rabuck, A. D.; Raghavachari, K.; Foresman, J. B.; Ortiz, J. V.; Cui, Q.; Baboul, A. G.; Clifford, S.; Cioslowski, J.; Stefanov, B. B.; Liu, G.; Liashenko, A.; Piskorz, P.; Komaromi, I.; Martin, R. L.; Fox, D. J.; Keith, T.; Al-Laham, M. A.; Peng, C. Y.; Nanayakkara, A.; Challacombe, M.; Gill, P. M. W.; Johnson, B.; Chen, W.; Wong, M. W.; Gonzalez, C.; Pople, J. A. *Gaussian 03*, revision B.04; Gaussian, Inc.: Wallingford, CT, 2004.

The reaction was stopped by closing the ethylene supply and cooling down the system to −70 °C. After the pressure in the reactor decreased to atmospheric pressure, the reaction was quenched by adding 1 mL of methanol. *n*-Heptane, used as internal standard, was also introduced and the mixture was analyzed by quantitative GC, calibrated with standard samples (except in the case of butenes for which the calibration was based upon the response factor of *n*-pentane).

Computational Details. Calculations were performed with the GAUSSIAN 03 series of programs.[29] DFT[30] was applied with the B3PW91 functional.[31,32] A quasi-relativistic effective core potential operator was used to represent the 10 innermost electrons of the nickel atom.[33] The basis set for the metal was that associated with the pseudo potential, with a standard double-ζ LANL2DZ contraction[33] completed by a set of polarization f functions (exponent = 1.472),[34] and the standard 6-31G* basis set was used for all the other atoms (C, N, O, P, and H). The stationary points were characterized as minima by full vibration frequencies calculations.

X-ray Crystallography for complexes 2, 5 and 6. Dark blue needles of **2** crystallized by slow diffusion of hexanes into a saturated dichloromethane solution of the complex. Green blocks of **5** crystallized by slow diffusion of toluene into a saturated dichloromethane solution of the complex. Brown blocks of **6** were obtained by diffusion of hexanes into a saturated dichloromethane solution of the complex. Data were collected on a Nonius Kappa CCD diffractometer using a Mo Kα ($\lambda = 0.71073$ Å) X-ray source and a graphite monochromator at 150 K. An additional experiment was conducted at room temperature for crystals of **2** but gave the same structure. Experimental details are described in Table 1. The crystal structures were solved using SIR 97[35] and SHELXL97.[36] ORTEP drawings were made using ORTEP III for Windows.[37] Crystallographic data can be obtained free of charge at www.ccdc.cam.ac.uk/conts/retrieving.html [or from the Cambridge Crystallographic Data Centre, 12 Union Road, Cambridge CB21EZ, UK; fax: (int) +44-1223/336-033 ; e-mail: deposit@ccdc.cam.ac.uk] with the deposition numbers CCDC 649846−649848, respectively, for **2**, **5**, and **6**.

Acknowledgment. The CNRS, the Ecole Polytechnique, the Institut Français du Pétrole, and the IDRIS (for computer time, project no. 171616) are thanked for supporting this work.

Supporting Information Available: Computational details, computed Cartesian coordinates, thermochemistry, energies, three lower frequencies of all theoretical structures, CIF files and tables giving crystallographic data for **2** and **5** (including atomic coordinates, bond lengths and angles, and anisotropic displacement parameters), and X-ray structure of **6** and its crystallographic data. This material is available free of charge via the Internet at http://pubs.acs.org.

IC701529A

(30) (a) Ziegler, T. *Chem. Rev.* **1991**, *91*, 651−667. (b) Parr, R. G.; Yang, W. *DFT*; Oxford University Press: Oxford, 1989.
(31) Becke, A. D. J. *J. Phys. Chem.* **1993**, *98*, 5648−5662.
(32) Perdew, J. P.; Wang, Y. *Phys. Rev. B* **1992**, *45*, 13244−13249.
(33) Hay, P. J.; Wadt, W. R. *J. Chem. Phys.* **1985**, *82*, 299−310.
(34) Ehlers, A.; Böhme, M.; Dapprich, S.; Gobbi, A.; Höllwarth, A.; Jonas, V.; Köhler, K. F.; Stegmann, R.; Veldkamp, A.; Frenking, G. *Chem. Phys. Lett.* **1993**, *208*, 111−114.
(35) Altomare, A.; Burla, M. C.; Camalli, M.; Cascarano, G.; Giacovazzo, C.; Guagliardi, A.; Moliterni, A. G. G.; Polidori, G.; Spagna, R. *J. Appl. Cryst.* **1999**, *32*, 115−119.
(36) Sheldrick, G. M. *SHELXL-97*; Universität Göttingen: Göttingen, Germany, 1997.
(37) Farrugia, L. J. *ORTEP-3*; Department of Chemistry: University of Glasgow, 2001.